Environmental Science & Technology

pubs.acs.org/est

Article

Enhancing the Thermal Mineralization of Perfluorooctanesulfonate on Granular Activated Carbon Using Alkali and Alkaline-Earth Metal Additives

Charbel Abou-Khalil, Liliya Chernysheva, Anthony Miller, Angela Abarca-Perez, Graham Peaslee, Pierre Herckes, Paul Westerhoff, and Kyle Doudrick*

Cite This: https://doi.org/10.1021/acs.est.3c09795

Read Online

ACCESS | Metrics & More | Article Recommendations | Supporting Information

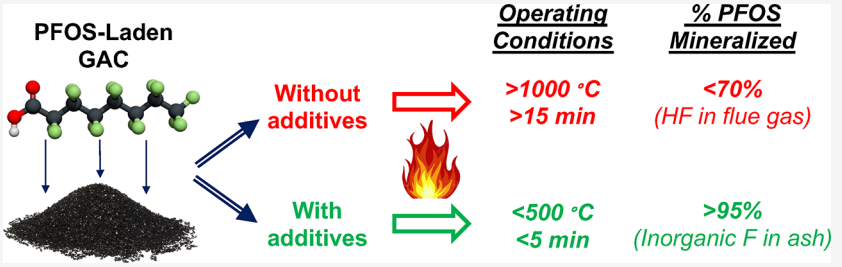

ABSTRACT: Thermal treatment has emerged as a promising approach for either the end-of-life treatment or regeneration of granular activated carbon (GAC) contaminated with per- and polyfluoroalkyl substances (PFAS). However, its effectiveness has been limited by the requirement for high temperatures, the generation of products of incomplete destruction, and the necessity to scrub HF in the flue gas. This study investigates the use of common alkali and alkaline-earth metal additives to enhance the mineralization of perfluorooctanesulfonate (PFOS) adsorbed onto GAC. When treated at 800 °C without an additive, only 49% of PFOS was mineralized to HF. All additives tested demonstrated improved mineralization, and $Ca(OH)_2$ had the best performance, achieving a mineralization efficiency of 98% in air or N_2. Its ability to increase the reaction rate and shift the byproduct selectivity suggests that its role may be catalytic. Moreover, additives reduced HF in the flue gas by instead reacting with the additive to form inorganic fluorine (e.g., CaF_2) in the starting waste material. A hypothesized reaction mechanism is proposed that involves the electron transfer from O^{2-} defect sites of CaO to intermediates formed during the thermal decomposition of PFOS. These findings advocate for the use of additives in the thermal treatment of GAC for disposal or reuse, with the potential to reduce operating costs and mitigate the environmental impact associated with incinerating PFAS-laden wastes.

KEYWORDS: *PFAS, PFOS, incineration, GAC, destruction*

INTRODUCTION

Per- and polyfluoroalkyl substances (PFAS) comprise a diverse group of synthetic organic compounds known for their exceptional thermal, chemical, and biological stability, water and oil resistance, and surfactant properties.[1] PFAS find application in various industrial and consumer products, such as aqueous film-forming foams (AFFFs), nonstick cookware, stain-resistant fabrics and carpets, some cosmetics, and water-repellent clothing, among others.[2] Due to their recalcitrance, PFAS are ubiquitous in the environment,[3−8] and they have been detected in municipal wastewater, freshwaters, and treated drinking water.[6,9,10] Consequently, there is a growing imperative to remediate PFAS-contaminated waters, driven by heightened societal and regulatory awareness amplified by advancing toxicology research on this class of contaminants.[11−14]

Conventional water treatment processes face limitations in effectively removing and destroying PFAS.[15,16] Adsorbents such as granular activated carbon (GAC) are an attractive prospect for removing PFAS from water due to the low cost.[16] However, managing spent adsorbents contaminated with PFAS poses a disposal challenge. The United States Environmental Protection Agency and the Department of Defense (DoD) have outlined interim guidance for handling PFAS-laden solids, suggesting landfilling, thermal reactivation, and incineration as potential methods.[17,18] Landfilling carries the risk of PFAS re-entering the environment,[19] making thermal treatment more practical for end-of-life destruction or regeneration of PFAS-contaminated GAC.[20−23] Yet, the thermal destruction of PFAS

Received: November 22, 2023
Revised: May 24, 2024
Accepted: May 28, 2024

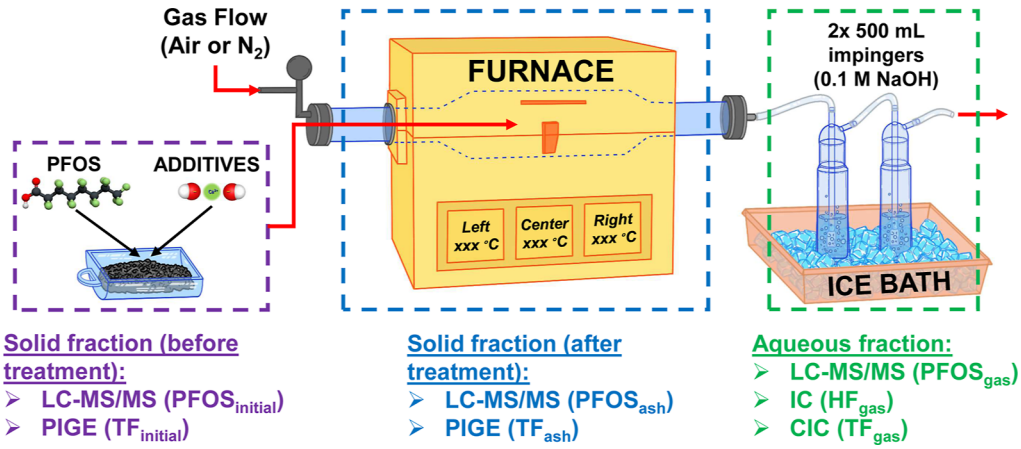

Figure 1. Schematic of the experimental setup, sampling, and analysis.

requires very high temperatures (>1000 °C) and it releases undesirable products of incomplete destruction (PIDs) in the flue gas.[15,24−26] As a result, the DoD has advised exercising caution in employing thermal treatment for managing PFAS wastes until further information is acquired.[17]

The incineration of PFAS-contaminated wastes might be enhanced by the incorporation of additives, potentially reducing the temperature and time required for mineralization while minimizing the generation of PIDs.[27−29] Recent research has highlighted the efficacy of calcium-based additives in augmenting PFAS mineralization at relatively low temperatures (<500 °C).[27−29] These investigations were conducted using a muffle furnace without air flow, and qualitative and (semi)-quantitative methods were used to track the fluorine mass balance. Of the calcium-based minerals examined, $Ca(OH)_2$ was the most efficient with respect to mineralization. Critical knowledge gaps remain for additive-assisted thermal treatment of PFAS, including the exploration of other alkali and alkaline-earth metals, the effect of the counterion, the quantitative fate of fluorine, the underlying mechanism driving the enhancement, and the effect of treatment duration. With regards to the counterion, several studies have also shown that hydroxides (e.g., NaOH) considerably enhance the degradation of PFAS during incineration,[30] hydrothermal liquefaction,[25,31,32] and low-temperature treatment in polar, nonprotic solvents.[33] This would suggest that both the metal and the hydroxide play a role in enhancing the mineralization of PFASs and mitigating PIDs.[20]

The aim of this study was to systematically explore the efficacy of alkali and alkaline-earth metal compounds in enhancing the mineralization of perfluorooctanesulfonate (PFOS) adsorbed onto GAC during thermal treatment. PFOS was chosen as a representative perfluorosulfonic acid due to its prevalence at numerous military installations, resulting from legacy AFFF usage,[34−39] historic use in consumer products,[40] and it being a common byproduct of various precursors.[41−44] Several variables were tested, including the alkali and alkaline-earth metal additive, treatment temperature, treatment time, the additive-to-fluorine molar ratio, and the presence/absence of oxygen. Additionally, unique to this study was the utilization of both total and target PFAS analyses to trace the fate of fluorine during thermal treatment. First, we present results with an accompanying discussion on the mineralization efficiency and distribution of the F byproducts. Then, using the outcomes of these experiments, we put forth a hypothesis that describes the possible catalytic mechanism that drives the thermal destruction of PFOS using additives. Finally, we provide insights into the implications of using additives in practice with a discussion of future needs.

METHODS

Preparation of PFOS-Contaminated GAC. A detailed description of the chemicals used in this study can be found in the Supporting Information (Section S1). PFOS stock solutions with a 100 mg/L concentration were prepared in 1 L Nalgene laboratory bottles (16127-226, VWR, PA, USA) by adding 100 mg of PFOS to 1 L of ultrapure Milli-Q water. The bottles were placed on a shaking table at 100 rpm for 24 h to ensure complete dissolution. GAC (F400, Carbon Calgon Corporation, PA, USA),[45] with a mean particle diameter of 1.0 mm and a surface area of 1050 m^2/g, was dried for 48 h at 60 °C in air. The calcium content of the dried GAC was determined by digesting 500 mg samples in triplicate in concentrated H_2SO_4 following the CEM MARS sixth method note.[46] The digestate was then analyzed for calcium using an Avio 200 inductively coupled plasma optical emission spectrometer (PerkinElmer, GA, USA).

The dried GAC was added to the PFOS stock solution bottles at 25 g/L to achieve a concentration of 4 mg PFOS/g GAC, which is less than the maximum adsorption capacity of GAC F400 when treating PFOS-contaminated waters.[47] The bottles were placed on a shaking table to mix the content at 100 rpm for 48 h. Then, the bottles were left stagnant for 24 h to allow the GAC to settle, after which it was collected and dried in an oven at 60 °C for 72 h. To confirm that the majority of PFOS was adsorbed onto the GAC, liquid samples were collected before and after shaking with GAC for subsequent analysis, which indicated that more than 99% of PFOS was adsorbed. In addition, the bottles were washed with a 0.1% NH_4OH/MeOH solution to quantify the amount of PFOS that adsorbed onto the walls. The wash was analyzed for PFOS by liquid chromatography with tandem mass spectrometry (LC−MS/MS; Agilent 6470B Triple Quadrupole LC−MS System, Agilent Technologies, DE, USA), which showed that there was no measurable PFOS detected in the wash within our detection limits (approximately 15 ng PFOS/L), implying that any PFOS loss to the walls of the bottles would have been <0.01%. The PFOS-contaminated GAC was poured into a 500 mL Nalgene bottle and then stored in a freezer at −20 °C. All

https://doi.org/10.1021/acs.est.3c09795
Environ. Sci. Technol. XXXX, XXX, XXX−XXX

experiments were conducted within 3 weeks of preparing the PFOS-contaminated GAC.

Thermal Treatment of GAC. A total of 36 runs from 6 experimental sets were conducted (Table SI-1). It should be noted that only the baseline and Run 2−6 (Table SI-1; same operating conditions as those of the baseline but without additives) were conducted in triplicate. Figure 1 displays a schematic of the experimental setup, sampling locations, and analytical procedures. Additives were added by mixing them with PFOS-contaminated GAC in 50 mL polypropylene tubes (05-539-9LC, Fisher Scientific, MI, USA) using a tube rotator (88-861-049, Fisher Scientific, MI, USA) at 30 rpm for 30 min. Four grams of contaminated GAC was poured into a laboratory-grade 50 mL quartz boat (Alpha Nanotech Inc., NC, USA) and then inserted into the tube furnace (OTF-1200X, MTI Corporation, CA, USA) after reaching the desired temperature. A less than 2 °C loss in temperature was observed from sample insertion. It should be noted that the thermocouples of this furnace measure the air temperature (i.e., above the sample) and not the temperature within the sample. Gas was flowed at a rate of 1.5 L/min (residence time of about 3.4 min in the tube furnace) from a gas cylinder using a mass flow controller (Alicat Scientific, AZ, USA). The gas was either air (Ultra Zero grade Air, American Welding and Gas, IN, USA) or N_2 (Ultra High Purity grade Nitrogen, American Welding and Gas, IN, USA). A gas flow rate of 1.5 L/min ensured that no HF was captured on the tube furnace or in any part of the setup used (i.e., inlet, tubing, etc.). This was tested by rinsing the entire system with 0.1 M NaOH solution and then measuring the rinsate for fluoride and PFAS. The gas flowed out from the furnace through 0.25″ stainless steel tubing (Smooth-Bore Seamless 316, McMaster-Carr, IL, USA) into two 500 mL glass impingers in series, each containing 200 mL of 0.1 M NaOH solution. To minimize the condensation of byproducts in the stainless steel tubing, it had a short length of 30 cm. The impingers, which were used to capture the soluble gas products (e.g., HF and soluble PIDs) produced during treatment, were placed in series and kept in an ice bath. After each run, the treated GAC—also referred to as ash, although most of the GAC (>80% by mass) remained intact after treatment (as detailed in the Supporting Information, Table SI-2)—was removed from the furnace, the furnace was sealed again, and then the gas flow was maintained for an additional 10 min to pass any remaining fluorine products through the system, resulting in a volume of 15 L of gas passed, which was more than two times the working volume of the system. The treated GAC sample was left to cool in a hood for 5 min before being weighed to determine the mass loss. It was then transferred into a 15 mL polypropylene tube (S50712, Fisher Scientific, MI, USA) and stored at −20 °C until analysis. The aqueous solutions from the impingers were poured into 50 mL polypropylene tubes (05-539-9LC, Fisher Scientific, MI, USA) and then stored at 4 °C.

The baseline run for GAC loaded with PFOS, from which all other experiments were varied, was selected as 800 °C, air, and with $Ca(OH)_2$ at a 1:1 Ca/F molar ratio (Table SI-1). The temperature of 800 °C was selected for the baseline since it is estimated to be the point at which more than 80% defluorination of PFSAs occurs.[24] Furthermore, this is the average temperature that hazardous waste incinerators commonly operate at in the rotary chamber.[48] $Ca(OH)_2$ was selected as the additive for the baseline since it has been previously shown to enhance the thermal treatment of PFOS.[28] From the baseline experiment, the effects of the additive type, operating temperature, presence of oxygen, treatment time, and additive-to-fluorine ratio were tested (Table SI-1).

A blank run, which consisted of GAC with no PFOS loaded, was treated at 800 °C in air for 15 min. This was done to verify that no fluorinated byproducts were generated by the GAC. In Experiment Set 1, several different additives were investigated, including $Ca(OH)_2$, CaO, $Ca_5(PO_4)_3(OH)$, $CaCl_2$, $CaCl_2$ + NaOH (i.e., mixture of $CaCl_2$ and NaOH in powder form), $Mg(OH)_2$, MgO, NaOH, NaCl, NH_4OH/H_2O (i.e., NH_4OH in solution), and HCl/H_2O (i.e., HCl in solution). The oxides and chlorides were investigated to determine the effect of hydroxide. NH_4OH/H_2O and HCl/H_2O were used as controls to explore the effect of OH/H_2O and H/H_2O additions without an alkali or alkaline-earth metal. Both NH_4OH/H_2O and HCl/H_2O were added to the PFOS-contaminated GAC as an aqueous solution, where select volumes were added from a stock solution (2500 mg/L). Unlike the other samples, these two were not dried prior to thermal treatment. The additive-to-fluorine molar ratio (X/F) used was 1:1 for X = Ca and Mg and 2:1 for X = Na, HCl/H_2O, and NH_4OH/H_2O. This corresponded to twice the stoichiometric requirement to form XF_n. In Experiment Sets 2 and 3, the effect of the furnace's operating temperature was investigated without and with $Ca(OH)_2$, respectively. In Experiment Set 4, the effect of oxygen was explored by using N_2 as the carrier gas. In Experiment Set 5, the effect of the treatment time was investigated at 500 and 800 °C (i) with $Ca(OH)_2$ from 5 to 30 min and (ii) without $Ca(OH)_2$ from 5 to 60 min. In Experiment Set 6, the effect of the Ca/F ratio was investigated from 0.5 to 8.0.

Analytical Procedures. To calculate the fluorine mass balance, we analyzed the initial loading of PFOS on GAC ($PFOS_{initial}$), the PFOS remaining on the GAC after incineration ($PFOS_{ash}$), the total fluorine on the GAC after incineration (TF_{ash}), the PFOS in the impingers after incineration ($PFOS_{gas}$), the total soluble fluorine in the impingers after incineration (TF_{gas}), and the HF in the impingers after incineration (HF_{gas}). The total inorganic fluorine on the GAC after incineration (IF_{ash}) was calculated by subtracting $PFOS_{ash}$ from TF_{ash}, and the total organic fluorine in the impingers after incineration (OF_{gas}) was calculated by subtracting HF_{gas} from TF_{gas}.

$PFOS_{initial}$ and $PFOS_{ash}$ were measured by LC−MS/MS following EPA method 1633 draft 4, modified for GAC (method details are presented in the Supporting Information, Section S3).[49] $PFOS_{initial}$ and $PFOS_{ash}$ were also measured using particle-induced gamma-ray emission (PIGE) spectrometry. The latter is generally used to analyze light elements such as lithium, boron, fluorine, aluminum, and silicon in a variety of solid matrices, and it has been successful in measuring fluorine in PFAS-laden solids with a detection limit of about 10 μg F per gram of dry solids.[50−52] The preparation of samples and standards for analysis by PIGE is detailed in the Supporting Information (Section S4, Figure SI-1). $PFOS_{gas}$ was measured by LC−MS/MS by diluting the impinger solution in methanol at an 80:20 ratio. HF_{gas} was measured using ion chromatography (IC; ECO IC, Metrohm, FL, USA). TF_{gas} was measured using combustion ion chromatography (CIC; Metrohm CIC, Metrohm, FL, USA) after concentrating the samples 5-fold using a blowdown evaporator (Biotage TurboVap LV, Biotage, NC, USA), whereby 10 mL samples

https://doi.org/10.1021/acs.est.3c09795
Environ. Sci. Technol. XXXX, XXX, XXX−XXX

were subject to a gentle nitrogen purge for 6 h in a water bath heated to 60 °C until a volume of 2 mL was reached. TF_{ash} was measured by PIGE spectrometry. IF_{ash} was calculated by subtracting $PFOS_{ash}$ from TF_{ash}. All samples tested by IC, CIC, LC−MS/MS, and PIGE were analyzed in triplicate. Analytical results were reported as the average ± standard deviation.

The fraction of fluorine mass that was recovered for each species (α_F), the total fraction of fluorine mass recovered ($\alpha_{F,total}$), and the fraction of the mass of PFOS that was mineralized were calculated using eqs 1−3, respectively.

$$\alpha_F\ (\%) = \frac{X_{mass}}{PFOS_{initial}} \times 100\%;$$

$$\text{where, } X_{mass} = PFOS_{ash},\ IF_{ash},\ HF_{gas},\ \text{or } OF_{gas} \quad (1)$$

$$\alpha_{F,total}\ (\%) = \frac{PFOS_{ash} + IF_{ash} + HF_{gas} + OF_{gas}}{PFOS_{initial}} \times 100\% \quad (2)$$

$$\text{mineralization efficiency}\ (\%) = \frac{IF_{ash} + HF_{gas}}{PFOS_{initial}} \times 100\% \quad (3)$$

Analytical Assumptions. Obtaining a total fluorine mass balance as discussed in the analytical procedures is challenging. It has limitations and requires some assumptions. First, for computing OF_{gas}, all fluorinated compounds captured in the impingers that were not HF were assumed to be organic. Other inorganic fluorine compounds, such as fluorosilicates, could form in the gas phase, but the hydrolysis of fluorosilicates to HF is known to occur rapidly and with a high equilibrium constant.[53] The full reaction has been shown to dissociate from HF at yields greater than 95% at much higher concentrations and at a pH lower than that of the impinger solutions. Therefore, in the alkaline impingers, and under favorable hydrolysis conditions, the number of fluorosilicates remaining would be small.

Second, IF_{ash} is calculated based on the assumption that all fluorine remaining on the treated GAC after the NH_4OH/methanol extraction is inorganic. However, nontargeted organic F and fluorinated PID radicals that reacted with GAC (e.g., forming CF_2 groups) could have remained on the treated GAC after extraction. This was accounted for by analyzing the fluorine remaining on the extracted GAC samples using PIGE and the chemical state of the products (e.g., C−F or Ca−F) using X-ray photoelectron spectroscopy (XPS) (method details are presented in the Supporting Information, Section S6).

Third, the extraction efficiency of targeted PFAS from GAC was assumed to be constant for all samples (i.e., to obtain $PFOS_{initial}$ and $PFOS_{ash}$). In spike-recovery experiments for the extraction of PFOS from triplicate samples, the recovery of PFOS was 97% ± 3.1% and 81% ± 3.4% for the control and GAC, respectively (Section S3). The latter recovery was used to adjust all extracted PFAS concentrations for the treated GAC. Analysis of extracted and nonextracted GAC samples by PIGE confirmed the LC−MS/MS results, with approximately 15−20% F remaining on the GAC after extraction.

RESULTS AND DISCUSSION

Effect of the Additive Type. Several additives were chosen to explore the effect of the alkali or alkaline-earth metal and the counterion on the thermal treatment of PFOS. Figure 2 displays the fraction of fluorine mass recovered (α_F) for different additives used to treat PFOS-contaminated GAC at

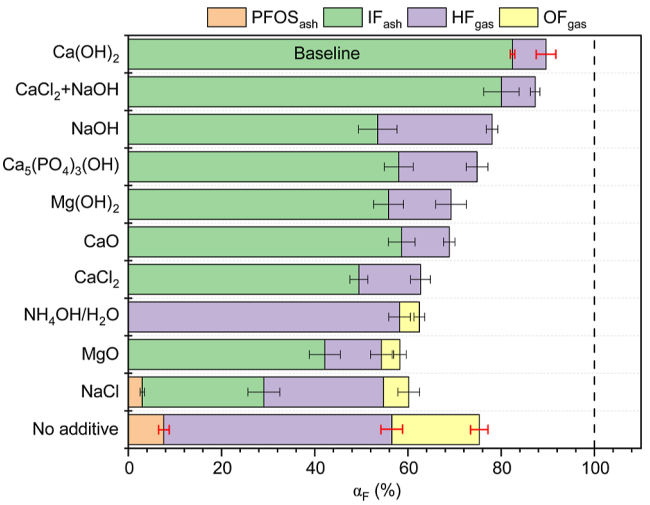

Figure 2. Fraction of fluorine mass recovered (α_F) for $PFOS_{ash}$, IF_{ash}, HF_{gas}, and OF_{gas} after treatment of PFOS-contaminated GAC at 800 °C in air (1.5 L/min) for 15 min with different additives. The X/F ratio was 1.0 for X = Ca and Mg and 2.0 for X = Na and NH_4OH/H_2O. The red error bars represent one standard deviation of triplicate runs, while the remaining error bars represent one standard deviation of analytical triplicates. The dashed line indicates 100% recovery of fluorine.

800 °C in air for 15 min. The data in Figure 2 is sorted from the highest to the lowest mineralization efficiency (eq 3). All alkali and alkaline-earth metals improved the mineralization efficiency compared to that when not using an additive, with Ca > Na > Mg. The hydroxide-based alkali and alkaline-earth metals—$Ca(OH)_2$, NaOH, $Mg(OH)_2$, and $Ca(PO_4)_3(OH)$—had a higher mineralization efficiency than that of the oxides and chlorides [$Ca(OH)_2$ > CaO > $CaCl_2$, NaOH > NaCl, and $Mg(OH)_2$ > MgO]. The mineralization efficiency for the additives used to probe the absence of the metal—NH_4OH/H_2O and HCl/H_2O—was lower than that of those containing a metal. The mineralization efficiency of NH_4OH/H_2O was slightly better than that with no additive (58 vs 49%) and all PFOS was removed from the GAC, whereas HCl/H_2O results were similar to those with no additive (not shown). The Ca, Na, and Mg additives will presumably form their respective XF_n products. For Ca, its product was confirmed by XPS analysis to be CaF_2 in the IF_{ash} (Figure SI-2).

Not only did the mineralization efficiency vary by additive but the distribution of the mineralized products (IF_{ash} and HF_{gas}) and PIDs also varied considerably (Tables SI-3 and SI-4). The IF_{ash}/HF_{gas} ratio was used as an indicator of how efficient the additive was at capturing HF as XF_n (e.g., CaF_2). The general trend in the IF_{ash}/HF_{gas} ratio was Ca > Mg > Na and OH > O > Cl, with the metal selection having the primary influence. For example, though NaOH (79%) was more effective than CaO (69%) and $CaCl_2$ (62%) at mineralizing PFOS, its IF_{ash}/HF_{gas} ratio (2.2) was lower than those of CaO (5.7) and $CaCl_2$ (3.7). Control experiments with pure NaF and CaF_2 (i.e., powder form with no GAC) at 800 °C did not produce notable (<5%) amounts of HF (not shown); thus, the lower IF_{ash}/HF_{gas} ratio for Na additives was unlikely due to the thermal decomposition of NaF to HF. NaCl was also the only metal-based additive that was unable to completely remove

https://doi.org/10.1021/acs.est.3c09795
Environ. Sci. Technol. XXXX, XXX, XXX−XXX

PFOS from GAC under the conditions tested. Its mineralization efficiency (55%) was comparable to that when not using additives (49%), suggesting only a minor enhancement, but it remained somewhat useful in capturing HF with an IF_{ash}/HF_{gas} ratio of 1.1.

In addition to capturing more HF_{gas} as IF_{ash}, the more active additives also reduced the missing F mass. No F was found in the post-treatment wash (with 0.1 M NaOH/methanol) of the system (i.e., quartz reactor, tubing, etc.), and no gas leaks were detected. Target analysis for 40 PFAS was conducted on the impinger solutions and the GAC ash, but none were detected (not including PFOS). Thus, the missing F mass was likely insoluble OF_{gas}, presumably volatile fluorocarbons that were either not captured by the impingers or not detected. This would include COF_2, C_2F_4, CF_4, and C_2F_6, which have been observed as gas-phase byproducts in previous studies on the thermal treatment of PFASs.[54] Thus, even at very high operating temperatures and at the residence time used (about 3 min), not all OF_{gas} (total) were mineralized to HF. Additional effort was made to capture the missing OF_{gas} as total F on a series of GAC emission capture beds (two 20 g beds in series) placed after the impingers, but no F was detected by PIGE analysis. This suggests that either GAC is not efficient at capturing the missing OF_{gas} or the mass is lower than the detection limit of PIGE. Beyond this study, additional development is needed to capture the volatile fluorocarbons on a solid-phase medium, which is required for PIGE analysis. It should be noted that while a nonpolar liquid phase coupled with CIC seems like an attractive option, this would not be suitable because these fluorocarbons are unable to be analyzed by CIC because they are thermally stable.

Due to the superior efficiency of $Ca(OH)_2$, this additive was chosen as the baseline additive and used in all subsequent experiments testing the operating temperature, treatment time, carrier gas, and Ca/F ratio.

Effect of the Operating Temperature. Figure 3 shows the fraction of fluorine mass recovered (α_F) for PFOS-contaminated GAC treated at varying temperatures in air (A) without and (B) with $Ca(OH)_2$. Given that the reported temperatures were the operating temperatures (i.e., air temperature) and not the temperatures within the solid matrix, localized temperatures where the reaction takes place may be higher (or lower). GAC has the potential to autoignite at temperatures >450 °C in air or inert atmospheres due to its oxygenated functional groups.[55] In this study, below 800 °C, we did not observe autoignition of the GAC. Above 800 °C, an observed reddish glow to the GAC indicated that either autoignition and/or smoldering might have occurred. This could increase the temperature of the GAC to up to 1000–1200 °C.[56−58] Nonetheless, even at 1000 °C and after 15 min of treatment, only about 20% mass loss of the GAC was observed (Table SI-2).

Without $Ca(OH)_2$, no mass loss of PFOS from the treated GAC (i.e., ash) was observed at 300 and 400 °C (Figure 3A). At 500 °C, ~41% of the total *F* mass remained as PFOS on the GAC ($PFOS_{ash}$), 20% was converted to HF_{gas}, and 21% was converted to OF_{gas} byproducts. With increasing temperature, the $PFOS_{ash}$ content continued to decrease, while HF_{gas} increased and OF_{gas} decreased proportionally, suggesting that increasing temperature facilitated the conversion of OF_{gas} products to HF_{gas}. This has been previously observed during the pyrolytic decomposition of PFOS.[56] This conversion of OF_{gas} to HF_{gas} was exponentially correlated (R^2 > 0.99), with

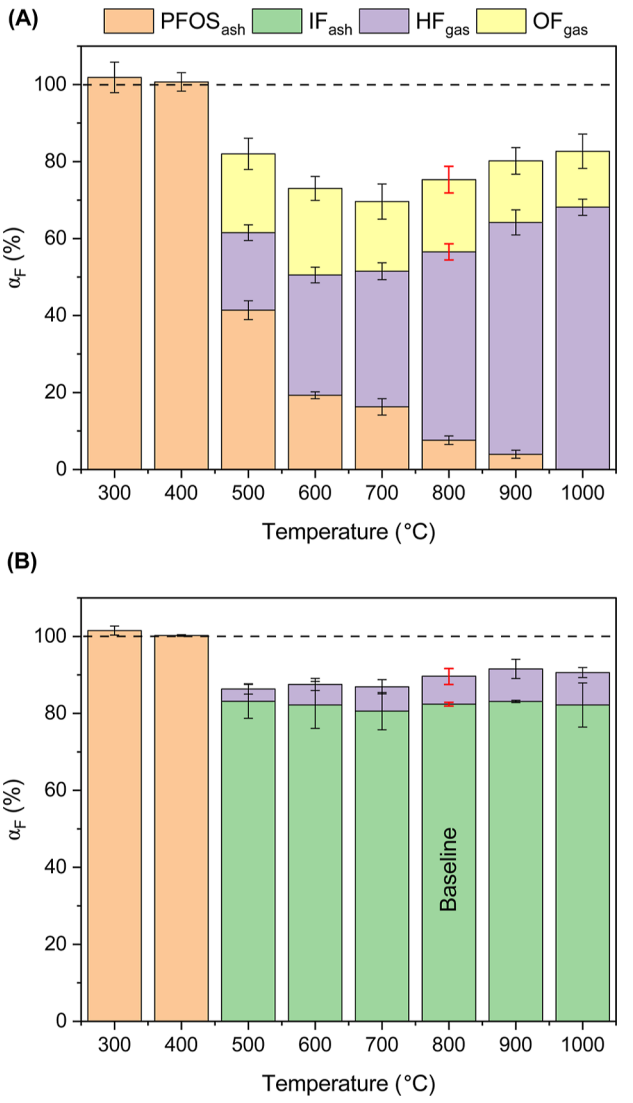

Figure 3. Fraction of fluorine mass recovered (α_F) for $PFOS_{ash}$, IF_{ash}, HF_{gas}, and OF_{gas} after the treatment of PFOS-contaminated GAC at varying temperatures in air (1.5 L/min) for 15 min (A) without $Ca(OH)_2$ and (B) with $Ca(OH)_2$. The Ca/F ratio was 1.0. The red error bars represent one standard deviation of triplicate runs, while the remaining error bars represent one standard deviation of analytical triplicates. The dashed line indicates 100% recovery of fluorine.

the HF_{gas}/OF_{gas} ratio increasing from 0.98 to 4.7 when increasing the temperature from 500 °C to 1000 °C (Figure SI-3). At 1000 °C, no PFOS remained on the GAC, but only 83% of the total F mass balance was accounted for as HF_{gas} (68%) and OF_{gas} (15%), with the remainder presumably being insoluble volatile fluorocarbons. It should be noted that no targeted PFAS were detected in the extracted samples, meaning that any fluorinated PIDs that might have remained on the treated GAC after washing were less than 0.25% of the total F mass balance. Moreover, if any organic F remained, it was not at a high enough concentration to be detected by XPS, which showed that the predominant form was CaF_2 (Figure SI-2).

Figure 3B shows the fraction of fluorine mass recovered (α_F) with the addition of $Ca(OH)_2$. Similar to the sample with no $Ca(OH)_2$ added, the initial mass loss of PFOS from GAC started at 500 °C with $Ca(OH)_2$, but the byproduct

https://doi.org/10.1021/acs.est.3c09795
Environ. Sci. Technol. XXXX, XXX, XXX−XXX

distribution was markedly different (Figure 3B). At this temperature, no $PFOS_{ash}$ was detected and 85% of the F mass was recovered as IF_{ash} (82%) and HF_{gas} (3%). No OF_{gas} was detected in the impingers with the addition of $Ca(OH)_2$. For all temperatures, the total fluorine mass recovered was between 85 and 103%, with slightly better recovery observed with increasing temperature. The addition of $Ca(OH)_2$ had a marked impact on the treatment of PFOS-laden GAC compared to that with no additive. It decreased the formation of PIDs, attenuated the formation of HF in the gas phase, and reduced the temperature required to achieve mineralization at the treatment time tested (15 min).

The baseline condition (800 °C, $Ca(OH)_2$ at 1:1 Ca/F, 15 min, air) was repeated with N_2 as an oxygen-free carrier gas instead of air. Compared to air conditions (IF_{ash} = 82%; HF_{gas} = 3%), the destruction of PFOS on GAC was slightly enhanced under pyrolytic conditions with a conversion of PFOS to IF_{ash} (87%), and no other products were detected. Typically, under pyrolysis conditions and at high temperatures without an additive, PFOS will decompose into PIDs.[24,57] The addition of $Ca(OH)_2$, however, significantly decreased the formation of PIDs under pyrolytic conditions. This outcome is promising since pyrolysis is favored for GAC regeneration,[20] and therefore, GAC could be reused after thermal treatment, even at regeneration at the lowest temperature where PFOS removal was observed (500 °C).

Mineralization Initiation Temperature. The conversion of PFAS to mineralized byproducts (i.e., IF_{ash} + HF_{gas}) is critical to establishing an efficient and sustainable thermal treatment process. In the absence of $Ca(OH)_2$, the mineralized byproduct was HF_{gas}, and in the presence of $Ca(OH)_2$, it was predominantly IF_{ash} with minor amounts of HF_{gas}. Figure 4 illustrates the mineralization efficiency of PFOS (i.e., computed using eq 3) with and without $Ca(OH)_2$ as a function of the operating temperature. Here, data from Figure 3 was collated with additional experiments conducted at 425, 450, and 475 °C to gain a better understanding of the temperature at which mineralization begins. The mineralization of PFOS was initiated between 425 and 450 °C with and without $Ca(OH)_2$, with a mineralization efficiency of 70 and 6.2%, respectively. Lower initiation temperatures have been observed for the destruction of PFOS during the thermal treatment of contaminated GAC and soil,[58] highlighting the importance of operating conditions when comparing results across studies. Though initiation temperatures with and without $Ca(OH)_2$ were similar, $Ca(OH)_2$ did enhance the amount of PFOS that was mineralized at 450 °C for a treatment time of 15 min.

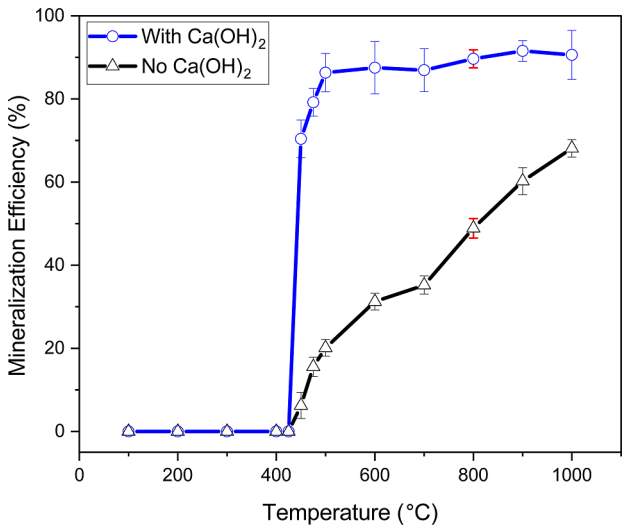

Figure 4. Mineralization efficiency as a function of temperature for the treatment of PFOS-contaminated GAC with and without $Ca(OH)_2$. Experiments were conducted in air (1.5 L/min) for 15 min. The red error bars represent one standard deviation of triplicate runs, while the remaining error bars represent one standard deviation of analytical triplicates. The mineralization efficiency was computed using eq 3.

Effect of the Treatment Time. As depicted in Figure 3A, PFOS was incompletely removed from GAC without $Ca(OH)_2$ until 1000 °C, but this may have been due to an insufficient treatment time (15 min) and not a temperature barrier. Herein, we explored the effect of treatment time to better understand how $Ca(OH)_2$ impacts the reaction. Figure 5 shows the fraction of fluorine mass recovered (α_F) for PFOS-contaminated GAC treated in air for varying treatment times without and with $Ca(OH)_2$ at 500 °C (Figure 5A) and 800 °C (Figure 5B). Samples were tested at 500 °C to investigate the impact of treatment time at the lowest temperature tested in Figure 3A at which PFOS mineralization occurred.

In the absence of $Ca(OH)_2$, increasing the treatment time from 5 to 60 min decreased $PFOS_{ash}$ while also increasing the fraction of HF_{gas} and OF_{gas}. $PFOS_{ash}$ was still 20% at a treatment time of 60 min at 500 °C, while at 800 °C, it was not detected. There was a positive log−log correlation (R^2 = 0.99) between the ratio of $PFOS_{ash}$ to HF_{gas} + OF_{gas} [$(PFOS_{ash}/(HF_{gas} + OF_{gas})$] and the treatment time, which indicates that increasing the treatment time would have diminishing returns with respect to PFOS removal from GAC. Both OF_{gas} and HF_{gas} increased by about 30−50% when increasing the time from 5 to 60 min.

With $Ca(OH)_2$, all PFOS was removed from the GAC after 5 min with a mineralization efficiency >85% for both operating temperatures. Similar treatment times were sufficient for the thermal treatment of PFOS in wastewater sludge amended with $Ca(OH)_2$.[29] Thus, not only does $Ca(OH)_2$ increase the mineralization efficiency at lower temperatures but it also reduces the treatment time required to do so. Reducing treatment times can potentially decrease the operating footprint and costs associated with the thermal treatment of PFAS-laden wastes.

Effect of the Ca/F Ratio. Figure 6 displays the fraction of fluorine mass recovered (α_F) at different Ca/F ratios using $Ca(OH)_2$. Using the theoretical stoichiometric Ca/F ratio of 0.5 resulted in incomplete mineralization of PFOS, forming HF_{gas} (20%) and OF_{gas} (8%), with the remainder of the mass that was missing (23%) being attributed to presumably volatile fluorocarbons. The most favorable treatment outcome was achieved at an excess stoichiometric Ca/F ratio of 2−4, resulting in >95% mineralization and fluorine mass recovery. The natural calcium concentration of the GAC (~1.42 mg/g, corresponding to a Ca/F ratio of ~0.25) did not seem to influence the thermal mineralization of PFOS since no IF_{ash} was detected in the experiments conducted without additives. There are a few reasons why an excess stoichiometric ratio would be needed, as discussed in the following section.

Proposed Reaction Mechanisms. Of all the additives tested, $Ca(OH)_2$ was the most efficient, with over 90% of PFOS being converted to mineralized byproducts for the

https://doi.org/10.1021/acs.est.3c09795
Environ. Sci. Technol. XXXX, XXX, XXX−XXX

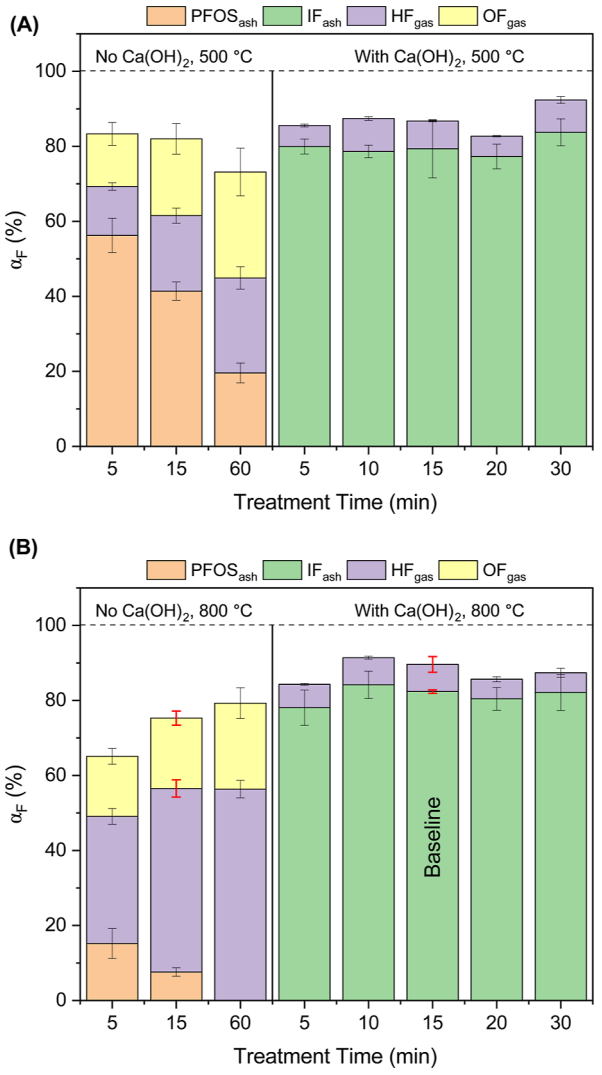

Figure 5. Fraction of fluorine mass recovered (α_F) for PFOS$_{ash}$, IF$_{ash}$, HF$_{gas}$, and OF$_{gas}$ after treatment of PFOS-contaminated GAC in air (1.5 L/min) for varying treatment times with and without Ca(OH)$_2$, at (A) 500 and (B) 800 °C, respectively. The Ca/F ratio was 1.0. The red error bars represent one standard deviation of triplicate runs, while the remaining error bars represent one standard deviation of analytical triplicates. The dashed line indicates 100% recovery of fluorine.

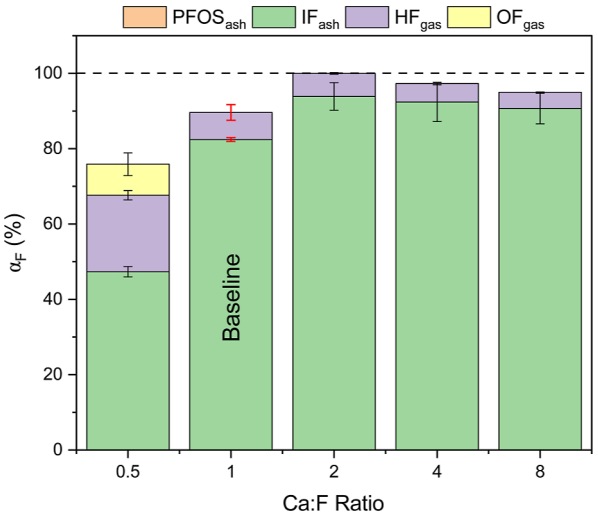

Figure 6. Fraction of fluorine mass recovered (α_F) for PFOS$_{ash}$, IF$_{ash}$, HF$_{gas}$, and OF$_{gas}$ after treatment of PFOS-contaminated GAC at 800 °C in air (1.5 L/min) for 15 min with varying Ca/F ratios using Ca(OH)$_2$. The red error bars represent one standard deviation of triplicate runs, while the remaining error bars represent one standard deviation of analytical triplicates. The dashed line indicates 100% recovery of fluorine.

conditions tested (Figure 2). Herein, we hypothesize that additives, or more specifically the metal oxide forms, served as a catalyst for at least one intermediate reaction, and additives with OH promoted the reaction through either the addition of basicity to the surface of additives, by altering the temperature at which the metal oxide forms, or through the release of H_2O. The catalytic activity of metal oxides has long been established,[59] and a few recent studies have already investigated their mineralization efficiencies and the mechanisms involved during the thermal treatment of PFAS.[27−29,60] Fully coordinated, pristine metal oxide surfaces are typically nonreactive, but the presence of defects exposes highly reactive basic (electron-donating) and acidic (electron-accepting) sites. With regards to the alkaline-earth metal oxides, much of the fundamental surface and catalysis science has focused on MgO.[61] In the 1960s, Tench and Nelson[62] used electron paramagnetic resonance (EPR) to prove that the defect sites of MgO have electron-donating capabilities. Electron transfer on defect-rich MgO can occur through two hypothesized processes.[61] The first is through O^{2-} ions located at edge, step, corner, and kink defect sites. These basic, low-coordinated sites are less stabilized (i.e., lower Madelung constant) than their bulk or surface counterparts. The resulting destabilized, occupied O 2p levels produce higher energy states in the band gap and serve as Lewis base sites that can directly transfer electrons to target compounds. The second is through the formation of O^{2-} vacancies in the bulk and at the surface. These vacancy defects, the so-called Farbzentren (F) centers, are surrounded by an array of Mg^{2+} cations and can trap excess electrons that can then transfer to chemisorbed molecules. Preparation of MgO with a high density of defects, often called "active" or "activated" MgO, can be done by pyrolyzing Mg(OH)$_2$ at temperatures between 400 and 850 °C.[63−69] Further treatment of this with hydrogen and irradiation produces oxygen vacancies, resulting in MgO with trapped electrons at F centers. Tench and Neslon[62] hypothesized that since they were using unirradiated MgO, the electron transfer mechanism was the direct transfer from lattice O^{2-} ions to adsorbed compounds, forming O^-. Several researchers have now confirmed this hypothesis through experimental and ab initio studies, proving that these low-coordinated O^{2-} sites serve as efficient reductive sites.[61]

The mechanisms of electron transfer from MgO translate to other oxides. In the case of CaO, it has a lower Madelung constant, which indicates lower stability of the O ions and thus a greater potential to donate electrons to target compounds.[61] Experiments with CO_2[70] and ab initio calculations[71] with CO_2 and SO_2 have confirmed the increased basicity and reactivity of CaO compared to MgO. In the processing of biofuels, CaO has been shown to be useful as a catalyst in deoxygenation, dehydrogenation, and cracking reactions.[72−80] In this study, both Ca(OH)$_2$ and CaO were more active than Mg(OH)$_2$ and MgO, thus aligning with previous observations and hypotheses. The differences in the mineralization efficiency and byproduct

https://doi.org/10.1021/acs.est.3c09795
Environ. Sci. Technol. XXXX, XXX, XXX−XXX

production of the Ca additives with varying counterions (OH, O, and Cl) can be partially explained by their respective decomposition temperatures. $Ca(OH)_2$ and $CaCl_2$ will thermally decompose to CaO between 400 and 500 °C[81] and between 600 and 800 °C,[82] respectively. In these experiments, the operating temperature was 800 °C; thus, the active material would be CaO. Differences observed between CaO and $CaCl_2$ may be due to the relatively high thermal stability of $CaCl_2$; thus, it may not have fully converted to CaO. Similar to the Ca compounds, NaOH and NaCl will decompose into Na_2O starting at 320 °C and >800 °C,[83] respectively, and $Mg(OH)_2$ will decompose into MgO between 300 and 400 °C. Presumably, Na_2O would have similar active sites as CaO and MgO. Interestingly, hydroxyapatite is stable up to 1000 °C,[84] yet the mineralization efficiency was similar to those of NaOH and $Mg(OH)_2$, which suggests a potentially different reaction pathway.

The results of this study, in conjunction with the prior published evidence, support the hypothesis that CaO, MgO, and Na_2O may be serving as a catalyst in at least one intermediate reaction of the thermal decomposition of PFOS. In this study, the key supporting results are that (1) CaO reduces the formation and selectivity of PIDs, improving the mineralization efficiency of PFOS (Figure 3), and (2) CaO increases the reaction rate for the decomposition of PFOS (Figure 5). A catalyst allows the reaction to proceed through a lower activation energy pathway for one or more reactions, thus increasing the overall reaction rate. Interestingly though, no effect on the initiation temperature of PFOS decomposition was observed (Figure 4). The catalytic activity of CaO would presumably occur at surface O^{2-} site defects that contain excess electrons. The requirement for a Ca/F ratio beyond the stoichiometric requirement of 0.5 (Figure 6) could be explained by either the need for more surface sites or catalyst poisoning. When HF is formed, it will react with CaO to form CaF_2, effectively poisoning the catalyst. Additionally, CO_2 and SO_2, once formed, can react with CaO to produce $CaCO_3$ and $CaSO_4$. While $CaCO_3$ starts to decompose to CaO below 800 °C,[85] $CaSO_4$ would remain stable at 800 °C.[86]

The reason for the improved performance of the hydroxides compared to that of the oxides and chlorides is potentially due to the addition of OH or H_2O to the reaction. All hydroxides tested in this study will release H_2O at 800 °C. In the absence of H_2O/OH, the thermal decomposition of the C−C bond in the presence of oxygen leads to several possible PIDs (e.g., CF_4, C_2F_6, COF_2, etc.).[24,26] On the other hand, H_2O has been shown to facilitate the reduction of these PIDs.[87,88] H_2O can also participate in hydrolysis reactions with intermediates, which may help to destabilize the alkyl chain and lead to C−C bond cleavage.[89] The effect of H_2O was partially evident in the NH_4OH/H_2O results (Figure 2), where adding H_2O/OH as an additive improved the decomposition of PFOS and altered the PID selectivity. Given that the results for $Ca(OH)_2$ and $CaCl_2$ + NaOH were similar, the CaO that is formed from $CaCl_2$ and the H_2O formed from NaOH are independent, and simply their presence in proximity is enough to facilitate the reactions.

The thermal destruction of PFOS is complex, involving several potential reaction pathways that are not yet well understood.[24] The reaction is further complicated with additives as they can provide alternative reaction pathways. In Figure SI-4, we outline a detailed reaction scheme for the thermal destruction of PFOS that was assembled from several sources of theoretical and experimental studies on the thermal destruction of PFOS,[90−97] perfluorooctanoic acid (PFOA),[98−101] trifluoroacetic acid,[102,103] and fluoroacetic acid.[104] Using prior results and those presented here, we hypothesize a possible reaction mechanism for $Ca(OH)_2$ and PFOS.

(1) Heating $Ca(OH)_2$ beyond 400 °C produces H_2O and activated CaO with O^{2-} and Ca^{2+}.

(2) Around 425 °C, thermolysis results in either the homolytic or heterolytic fragmentation of the sulfonic headgroup (reactions 1−3). Sulfonic acid is a good leaving group; thus, the heterolytic pathway to form a perfluoro carbocation seems plausible (reaction 2), but ab initio calculations suggest that the pathway is homolytic for PFOS (reaction 3),[90] forming $C_8F_{17}^{\bullet}$ and $^{\bullet}SO_3H$. For PFOA, ab initio calculations and experimental evidence have suggested a heterolytic pathway to form a perfluoro carbanion and SO_3 (reaction 1).[99] Alternatively, in the presence of CaO with O^{2-} defect sites and H_2O, electrons can directly cleave the α C−F to form F^- and C−H (so-called H/F exchange), which then forms a CH_2 carbene and shorter-chain PFAS, which repeats until the PFOS is fully mineralized.

(3) For $^{\bullet}C_8F_{17}$, several reaction pathways are possible (reaction [G]), forming various byproducts, including $^{\bullet}F$, CF_2, $^{\bullet}CF_3$, C_2F_4, CH_3F, COF_2, CH_4, CO, CO_2, trifluoroacetic acid, fluoroacetic acid, shorter-chain PFAS, perfluoro alcohols, and perfluoroalkenes. Several of these radicals have been observed experimentally for PFOS and PFOA.[95,101] For any of these intermediate reactions, the transfer of excess electrons from CaO could result in a more favorable pathway by eliminating the formation of radicals and forming F^- instead. At any point, radicals may react with the now electron-deficient O^{2-} site of CaO to complete the catalytic cycle. For example, $^{\bullet}C_8F_{17}$ could react with surface O^- to form O^{2-} and $^{+}C_8F_{17}$ (followed by reaction [F]). Additionally, Ca^{2+} defect sites may also play a role as strong electron acceptors or through their ability to form coordination bonds (i.e., chelation). Moreover, several of the proposed reactions are more favorable in the presence of excess H_2O, which may explain the more efficient performance of the metal hydroxides.

(4) The majority of HF that forms reacts with CaO to form CaF_2, effectively poisoning the catalyst.

Collectively, the results of this study suggest that $Ca(OH)_2$ is thermally decomposed to CaO, which may act as a catalyst through several different pathways, and H_2O, which may promote the decomposition of PFOS and PIDs. The reactions are complex, and a deeper understanding of the mechanisms, as well as providing more concrete evidence on the catalytic activity of CaO, will require a more detailed study that involves experimental evidence of electron transfer from the CaO (e.g., EPR spectroscopy analysis) combined with ab initio calculations.

Implications for Treatment of PFAS-Contaminated Wastes. $Ca(OH)_2$ is an economical chemical already utilized in the hazardous waste incineration industry for scrubbing acidic gases like HF or HCl. Hence, its integration into waste before treatment seems feasible, though it would require some forethought on how best to do that. In this study, the addition

https://doi.org/10.1021/acs.est.3c09795
Environ. Sci. Technol. XXXX, XXX, XXX−XXX

of $Ca(OH)_2$ showcased significant improvements in the thermal treatment of PFOS on GAC in multiple ways: it increased the reaction rate and thus lowered the temperature required to mineralize PFOS in a sufficient amount of time, it shifted more of the byproduct selectivity to HF, and it captured HF to form innocuous inorganic fluorine minerals in the treated waste. The change in the reaction pathway and the accelerated rate suggest that CaO functions as a catalyst. However, numerous questions remain unanswered. First, concerning mechanisms, a deeper exploration of the roles of the alkali and alkaline-earth metals and counterions is essential. A clearer understanding could pave the way for developing even more efficient catalysts. Advanced quantum chemical calculations could be used to provide mechanistic insights into the thermal decomposition and mineralization of PFAS, with and without additives.[105−109] Second, while CaO effectively enhanced the thermal decomposition of PFOS, its effectiveness on other PFAS variants with differing head groups, tail lengths, and fluorination degrees requires further exploration. Third, the urgent need persists for developing on- or off-line analytical methods capable of measuring the total fluorine of the gas-phase fluorocarbon byproducts. Present collection methods, such as thermal desorption tubes or canisters, are mostly reserved for specific target and nontarget analyses that may require tedious analysis or lack analytical standards. Also, while the addition of $Ca(OH)_2$ improved the mineralization of PFOS on GAC at low temperatures and in the absence of oxygen (i.e., regeneration), further studies are needed to confirm that GAC treated in such a way can be reused for drinking water treatment applications. Finally, as experiments have been confined to the bench scale, further investigations are essential to assess the scalability and economic viability of using such additives.

■ ASSOCIATED CONTENT

Supporting Information

The Supporting Information is available free of charge at https://pubs.acs.org/doi/10.1021/acs.est.3c09795.

> Materials, experimental runs conducted, description of the modified EPA 1633 method and recoveries, PIGE standardization and analysis, mass loss of GAC at different temperatures, XPS data, raw data, variation of HF_{gas}/OF_{gas} for Experiment 2, and possible reaction pathways for the thermal destruction of some PFOS (PDF)

■ AUTHOR INFORMATION

Corresponding Author

Kyle Doudrick − *Department of Civil and Environmental Engineering and Earth Sciences, University of Notre Dame, Notre Dame, Indiana 46556, United States;* orcid.org/0000-0003-1912-9819; Email: kdoudrick@nd.edu

Authors

Charbel Abou-Khalil − *Department of Civil and Environmental Engineering and Earth Sciences, University of Notre Dame, Notre Dame, Indiana 46556, United States;* orcid.org/0000-0002-2379-9551

Liliya Chernysheva − *Department of Civil and Environmental Engineering and Earth Sciences, University of Notre Dame, Notre Dame, Indiana 46556, United States*

Anthony Miller − *Department of Physics, University of Notre Dame, Notre Dame, Indiana 46556, United States;* orcid.org/0000-0001-8866-7595

Angela Abarca-Perez − *Department of Civil and Environmental Engineering and Earth Sciences, University of Notre Dame, Notre Dame, Indiana 46556, United States;* orcid.org/0000-0001-9139-7995

Graham Peaslee − *Department of Physics, University of Notre Dame, Notre Dame, Indiana 46556, United States;* orcid.org/0000-0001-6311-648X

Pierre Herckes − *School of Molecular Sciences, Arizona State University, Tempe, Arizona 85287, United States;* orcid.org/0000-0002-0205-3187

Paul Westerhoff − *School of Sustainable Engineering and the Built Environment, Arizona State University, Tempe, Arizona 85287, United States;* orcid.org/0000-0002-9241-8759

Complete contact information is available at: https://pubs.acs.org/10.1021/acs.est.3c09795

Author Contributions

Charbel Abou-Khalil: writing—original draft, data curation, investigation, and visualization. **Liliya Chernysheva**: data curation and visualization. **Tony Miller**: investigation. **Angela Abarca Perez**: investigation and visualization. **Graham Peaslee**: writing—editing. **Paul Westerhoff:** writing—editing. **Kyle Doudrick**: conceptualization, funding acquisition, supervision, and writing—review and editing.

Notes

The authors declare no competing financial interest.

■ ACKNOWLEDGMENTS

This research was funded by the Strategic Environmental Research and Development Program (SERDP) project ER21-1107. Dr. Abou-Khalil thanks the Environmental Change Initiative (ECI) at the University of Notre Dame for providing him with a fellowship to partially support his assignment as a postdoctoral research associate. We thank the Materials Characterization Facility (MCF), the Center of Environmental Science and Technology (CEST), and the Mass Spectrometry and Proteomics Facility (MSPF) at the University of Notre Dame for providing access to the appropriate analytical instruments that made this research possible.

■ REFERENCES

(1) Buck, R. C.; Franklin, J.; Berger, U.; Conder, J. M.; Cousins, I. T.; de Voogt, P.; Jensen, A. A.; Kannan, K.; Mabury, S. A.; van Leeuwen, S. P. J. Perfluoroalkyl and Polyfluoroalkyl Substances in the Environment: Terminology, Classification, and Origins. *Integr. Environ. Assess. Manage.* **2011**, *7* (4), 513−541.

(2) Glüge, J.; Scheringer, M.; Cousins, I. T.; Dewitt, J. C.; Goldenman, G.; Herzke, D.; Lohmann, R.; Ng, C. A.; Trier, X.; Wang, Z. An Overview of the Uses of Per- And Polyfluoroalkyl Substances (PFAS). *Environ. Sci.: Processes Impacts* **2020**, *22* (12), 2345−2373.

(3) Sáez, M.; De Voogt, P.; Parsons, J. R. Persistence of Perfluoroalkylated Substances in Closed Bottle Tests with Municipal Sewage Sludge. *Environ. Sci. Pollut. Res.* **2008**, *15* (6), 472−477.

(4) Cousins, I. T.; Dewitt, J. C.; Glüge, J.; Goldenman, G.; Herzke, D.; Lohmann, R.; Ng, C. A.; Scheringer, M.; Wang, Z. The High Persistence of PFAS Is Sufficient for Their Management as a Chemical Class. *Environmental Science: Processes and Impacts* **2020**, *22*, 2307−2312.

(5) Kahn, L. G.; Harley, K. G.; Siegel, E. L.; Zhu, Y.; Factor-Litvak, P.; Porucznik, C. A.; Klein-Fedyshin, M.; Hipwell, A. E. Persistent

Organic Pollutants and Couple Fecundability: A Systematic Review. *Hum. Reprod. Update* **2021**, *27*, 339−366.
(6) Crone, B. C.; Speth, T. F.; Wahman, D. G.; Smith, S. J.; Abulikemu, G.; Kleiner, E. J.; Pressman, J. G. Occurrence of Per- and Polyfluoroalkyl Substances (PFAS) in Source Water and Their Treatment in Drinking Water. *Crit. Rev. Environ. Sci. Technol.* **2019**, *49* (24), 2359−2396.
(7) Abou-Khalil, C.; Sarkar, D.; Braykaa, P.; Boufadel, M. C. Mobilization of Per- and Polyfluoroalkyl Substances (PFAS) in Soils: A Review. *Curr. Pollut. Rep.* **2022**, *8*, 422−444.
(8) Abunada, Z.; Alazaiza, M. Y. D.; Bashir, M. J. K. An Overview of Per-and Polyfluoroalkyl Substances (Pfas) in the Environment: Source, Fate, Risk and Regulations. *Water* **2020**, *12*, 3590.
(9) Lenka, S. P.; Kah, M.; Padhye, L. P. A Review of the Occurrence, Transformation, and Removal of Poly- and Perfluoroalkyl Substances (PFAS) in Wastewater Treatment Plants. *Water Res.* **2021**, *199*, 117187.
(10) Xu, B.; Liu, S.; Zhou, J. L.; Zheng, C.; Weifeng, J.; Chen, B.; Zhang, T.; Qiu, W. PFAS and Their Substitutes in Groundwater: Occurrence, Transformation and Remediation. *J. Hazard. Mater.* **2021**, *412*, 125159.
(11) Gaballah, S.; Swank, A.; Sobus, J. R.; Howey, X. M.; Schmid, J.; Catron, T.; McCord, J.; Hines, E.; Strynar, M.; Tal, T. Evaluation of Developmental Toxicity, Developmental Neurotoxicity, and Tissue Dose in Zebrafish Exposed to GenX and Other PFAS. *Environ. Health Perspect.* **2020**, *128* (4), 47005.
(12) McCarthy, C. J.; Roark, S. A.; Middleton, E. T. Considerations for Toxicity Experiments and Risk Assessments with PFAS Mixtures. *Integr. Environ. Assess. Manage.* **2021**, *17* (4), 697−704.
(13) Fenton, S. E.; Ducatman, A.; Boobis, A.; DeWitt, J. C.; Lau, C.; Ng, C.; Smith, J. S.; Roberts, S. M. Per- and Polyfluoroalkyl Substance Toxicity and Human Health Review: Current State of Knowledge and Strategies for Informing Future Research. *Environ. Toxicol. Chem.* **2021**, *40*, 606−630.
(14) Jane L Espartero, L.; Yamada, M.; Ford, J.; Owens, G.; Prow, T.; Juhasz, A. Health-Related Toxicity of Emerging per- and Polyfluoroalkyl Substances: Comparison to Legacy PFOS and PFOA. *Environ. Res.* **2022**, *212*, 113431.
(15) Winchell, L. J.; Wells, M. J. M.; Ross, J. J.; Fonoll, X.; Norton, J. W.; Kuplicki, S.; Khan, M.; Bell, K. Y. Per- and Polyfluoroalkyl Substances Presence, Pathways, and Cycling through Drinking Water and Wastewater Treatment. *J. Environ. Eng.* **2022**, *148* (1), 151003.
(16) Yadav, S.; Ibrar, I.; Al-Juboori, R. A.; Singh, L.; Ganbat, N.; Kazwini, T.; Karbassiyazdi, E.; Samal, A. K.; Subbiah, S.; Altaee, A. Updated Review on Emerging Technologies for PFAS Contaminated Water Treatment. *Chem. Eng. Res. Des.* **2022**, *182*, 667−700.
(17) DoD. *Interim Guidance on Destruction or Disposal of Materials Containing Per- and Polyfluoroalkyl Substances in the United States*; 2023. https://www.acq.osd.mil/eie/eer/ecc/pfas/docs/news/Memorandum_for_Interim_Guidance_on_Destruction_or_Disposal_of_Materials_Containing_PFAS_in_the_U.S.pdf.
(18) USEPA. *Interim Guidance on the Destruction and Disposal of Perfluoroalkyl and Polyfluoroalkyl Substances and Materials Containing Perfluoroalkyl and Polyfluoroalkyl Substances*; 2020. https://www.epa.gov/system/files/documents/2021-11/epa-hq-olem-2020-0527-0002_content.pdf (accessed 2023−09−16).
(19) Lu, J.; Lu, H.; Liang, D.; Feng, S. S.; Li, Y.; Li, J. A Review of the Occurrence, Monitoring, and Removal Technologies for the Remediation of per- and Polyfluoroalkyl Substances (PFAS) from Landfill Leachate. *Chemosphere* **2023**, *332*, 138824.
(20) Sonmez Baghirzade, B.; Zhang, Y.; Reuther, J. F.; Saleh, N. B.; Venkatesan, A. K.; Apul, O. G. Thermal Regeneration of Spent Granular Activated Carbon Presents an Opportunity to Break the Forever PFAS Cycle. *Environ. Sci. Technol.* **2021**, *55* (9), 5608−5619.
(21) Zgonc, D.; Ramos, P.; Gao, Y.; Hoek, E. M. V.; Blotevogel, J.; Rappé, A. K.; Mahendra, S. Hot Topic: Thermal Treatment of per- and Polyfluoroalkyl Substances. *Curr. Opin. Chem. Eng.* **2023**, *42*, 100976.
(22) Xiao, F.; Sasi, P. C.; Yao, B.; Kubátová, A.; Golovko, S. A.; Golovko, M. Y.; Soli, D. Thermal Stability and Decomposition of Perfluoroalkyl Substances on Spent Granular Activated Carbon. *Environ. Sci. Technol. Lett.* **2020**, *7* (5), 343−350.
(23) Verma, S.; Lee, T.; Sahle-Demessie, E.; Ateia, M.; Nadagouda, M. N. Recent Advances on PFAS Degradation via Thermal and Nonthermal Methods. *Chem. Eng. J. Adv.* **2023**, *13*, 100421.
(24) Wang, J.; Lin, Z.; He, X.; Song, M.; Westerhoff, P.; Doudrick, K.; Hanigan, D. Critical Review of Thermal Decomposition of Per- and Polyfluoroalkyl Substances: Mechanisms and Implications for Thermal Treatment Processes. *Environ. Sci. Technol.* **2022**, *56*, 5355−5370.
(25) Kumar, R.; Dada, T. K.; Whelan, A.; Cannon, P.; Sheehan, M.; Reeves, L.; Antunes, E. Microbial and Thermal Treatment Techniques for Degradation of PFAS in Biosolids: A Focus on Degradation Mechanisms and Pathways. *J. Hazard. Mater.* **2023**, *452*, 131212.
(26) Shields, E. P.; Krug, J. D.; Roberson, W. R.; Jackson, S. R.; Smeltz, M. G.; Allen, M. R.; Burnette, R. P.; Nash, J. T.; Virtaranta, L.; Preston, W.; Liberatore, H. K.; Wallace, M. A. G.; Ryan, J. V.; Kariher, P. H.; Lemieux, P. M.; Linak, W. P. Pilot-Scale Thermal Destruction of Per- and Polyfluoroalkyl Substances in a Legacy Aqueous Film Forming Foam. *ACS ES&T Eng.* **2023**, *3*, 1308−1317.
(27) Wang, F.; Lu, X.; Shih, K.; Liu, C. Influence of Calcium Hydroxide on the Fate of Perfluorooctanesulfonate under Thermal Conditions. *J. Hazard. Mater.* **2011**, *192* (3), 1067−1071.
(28) Wang, F.; Lu, X.; Li, X. Y.; Shih, K. Effectiveness and Mechanisms of Defluorination of Perfluorinated Alkyl Substances by Calcium Compounds during Waste Thermal Treatment. *Environ. Sci. Technol.* **2015**, *49* (9), 5672−5680.
(29) Wang, F.; Shih, K.; Lu, X.; Liu, C. Mineralization Behavior of Fluorine in Perfluorooctanesulfonate (PFOS) during Thermal Treatment of Lime-Conditioned Sludge. *Environ. Sci. Technol.* **2013**, *47* (6), 2621−2627.
(30) Watanabe, N.; Takata, M.; Takemine, S.; Yamamoto, K. Thermal Mineralization Behavior of PFOA, PFHxA, and PFOS during Reactivation of Granular Activated Carbon (GAC) in Nitrogen Atmosphere. *Environ. Sci. Pollut. Res.* **2018**, *25* (8), 7200−7205.
(31) Zhang, W.; Liang, Y. Effects of Hydrothermal Treatments on Destruction of Per- and Polyfluoroalkyl Substances in Sewage Sludge. *Environ. Pollut.* **2021**, *285*, 117276.
(32) Zhang, W.; Liang, Y. Hydrothermal Liquefaction of Sewage Sludge - Effect of Four Reagents on Relevant Parameters Related to Biocrude and PFAS. *J. Environ. Chem. Eng.* **2022**, *10* (1), 107092.
(33) Trang, B.; Li, Y.; Xue, X.-S.; Ateia, M.; Houk, K. N.; Dichtel, W. R. Low-Temperature Mineralization of Perfluorocarboxylic Acids. *Science* **2022**, *377* (6608), 839−845. https://www.science.org
(34) Longpré, D.; Lorusso, L.; Levicki, C.; Carrier, R.; Cureton, P. PFOS, PFOA, LC-PFCAS, and Certain Other PFAS: A Focus on Canadian Guidelines and Guidance for Contaminated Sites Management. *Environ. Technol. Innovation* **2020**, *18*, 100752.
(35) Arias E, V. A.; Mallavarapu, M.; Naidu, R.; Naidu, R. Identification of the Source of PFOS and PFOA Contamination at a Military Air Base Site. *Environ. Monit. Assess.* **2015**, *187* (1), 4111.
(36) Kärrman, A.; Elgh-Dalgren, K.; Lafossas, C.; Møskeland, T. Environmental Levels and Distribution of Structural Isomers of Perfluoroalkyl Acids after Aqueous Fire-Fighting Foam (AFFF) Contamination. *Environ. Chem.* **2011**, *8* (4), 372−380.
(37) De Solla, S. R.; De Silva, A. O.; Letcher, R. J. Highly Elevated Levels of Perfluorooctane Sulfonate and Other Perfluorinated Acids Found in Biota and Surface Water Downstream of an International Airport, Hamilton, Ontario, Canada. *Environ. Int.* **2012**, *39* (1), 19−26.
(38) Filipovic, M.; Woldegiorgis, A.; Norström, K.; Bibi, M.; Lindberg, M.; Österås, A. H. Historical Usage of Aqueous Film Forming Foam: A Case Study of the Widespread Distribution of Perfluoroalkyl Acids from a Military Airport to Groundwater, Lakes, Soils and Fish. *Chemosphere* **2015**, *129*, 39−45.

https://doi.org/10.1021/acs.est.3c09795
Environ. Sci. Technol. XXXX, XXX, XXX−XXX

(39) Hu, X. C.; Andrews, D. Q.; Lindstrom, A. B.; Bruton, T. A.; Schaider, L. A.; Grandjean, P.; Lohmann, R.; Carignan, C. C.; Blum, A.; Balan, S. A.; Higgins, C. P.; Sunderland, E. M. Detection of Poly- and Perfluoroalkyl Substances (PFASs) in U.S. Drinking Water Linked to Industrial Sites, Military Fire Training Areas, and Wastewater Treatment Plants. *Environ. Sci. Technol. Lett.* **2016**, *3* (10), 344−350.
(40) Van Asselt, E. D.; Rietra, R. P. J. J.; Römkens, P.; Van Der Fels-Klerx, H. J. Perfluorooctane Sulphonate (PFOS) throughout the Food Production Chain. *Food Chem.* **2011**, *128*, 1−6.
(41) Yu, N.; Shi, W.; Zhang, B.; Su, G.; Feng, J.; Zhang, X.; Wei, S.; Yu, H. Occurrence of Perfluoroalkyl Acids Including Perfluorooctane Sulfonate Isomers in Huai River Basin and Taihu Lake in Jiangsu Province, China. *Environ. Sci. Technol.* **2013**, *47* (2), 710−717.
(42) Wang, Y.; Arsenault, G.; Riddell, N.; Mccrindle, R.; Mcalees, A.; Martin, J. W. Perfluorooctane Sulfonate (PFOS) Precursors Can Be Metabolized Enantioselectively: Principle for a New PFOS Source Tracking Tool. *Environ. Sci. Technol.* **2009**, *43* (21), 8283−8289.
(43) Jackson, D. A.; Mabury, S. A. Polyfluorinated Amides as a Historical PFCA Source by Electrochemical Fluorination of Alkyl Sulfonyl Fluorides. *Environ. Sci. Technol.* **2013**, *47* (1), 382−389.
(44) Evich, M. G.; Davis, M. J. B.; McCord, J. P.; Acrey, B.; Awkerman, J. A.; Knappe, D. R. U.; Lindstrom, A. B.; Speth, T. F.; Tebes-Stevens, C.; Strynar, M. J.; Wang, Z.; Weber, E. J.; Henderson, W. M.; Washington, J. W. Per- and Polyfluoroalkyl Substances in the Environment. *Science* **2022**, *375* (6580), No. eabg9065.
(45) Calgon Carbon. Filrasorb400. https://www.calgoncarbon.com/app/uploads/F400-Secured.pdf (accessed Aug 02, 2023).
(46) Mars Method Note; Microwave Digestion of Activated Carbon. https://cemcontenttype.s3.amazonaws.com/content/media-library/attachments/MetNote_MARS6_Activated_Carbon_iPrep.pdf (accessed Aug 02, 2023).
(47) Senevirathna, S. T. M. L. D.; Tanaka, S.; Fujii, S.; Kunacheva, C.; Harada, H.; Shivakoti, B. R.; Okamoto, R. A Comparative Study of Adsorption of Perfluorooctane Sulfonate (PFOS) onto Granular Activated Carbon, Ion-Exchange Polymers and Non-Ion-Exchange Polymers. *Chemosphere* **2010**, *80* (6), 647−651.
(48) Oppelt, E. T. Incineration Of Hazardous Waste. *J. Air Pollut. Control Assoc.* **1987**, *37* (5), 558−586.
(49) USEPA. *Analysis of Per- and Polyfluoroalkyl Substances (PFAS) in Aqueous, Solid, Biosolids, and Tissue Samples by LC-MS/MS*; 2023. https://www.epa.gov/system/files/documents/2022-12/3rd%20Draft%20Method%201633%20December%202022%2012-20-22_508.pdf (accessed 2023−08−02).
(50) Peaslee, G. F.; Wilkinson, J. T.; McGuinness, S. R.; Tighe, M.; Caterisano, N.; Lee, S.; Gonzales, A.; Roddy, M.; Mills, S.; Mitchell, K. Another Pathway for Firefighter Exposure to Per- A Nd Polyfluoroalkyl Substances: Firefighter Textiles. *Environ. Sci. Technol. Lett.* **2020**, *7* (8), 594−599.
(51) Ritter, E. E.; Dickinson, M. E.; Harron, J. P.; Lunderberg, D. M.; DeYoung, P. A.; Robel, A. E.; Field, J. A.; Peaslee, G. F. PIGE as a Screening Tool for Per- and Polyfluorinated Substances in Papers and Textiles. *Nucl. Instrum. Methods Phys. Res., Sect. B* **2017**, *407*, 47−54.
(52) Whitehead, H. D.; Venier, M.; Wu, Y.; Eastman, E.; Urbanik, S.; Diamond, M. L.; Shalin, A.; Schwartz-Narbonne, H.; Bruton, T. A.; Blum, A.; Wang, Z.; Green, M.; Tighe, M.; Wilkinson, J. T.; McGuinness, S.; Peaslee, G. F. Fluorinated Compounds in North American Cosmetics. *Environ. Sci. Technol. Lett.* **2021**, *8* (7), 538−544.
(53) Crosby, N. T. EQUILIBRIA OF FLUOROSILICATE SOLUTIONS WITH SPECIAL REFERENCE TO THE FLUORIDATION OF PUBLIC WATER SUPPLIES. *J. Appl. Chem.* **1969**, *19* (4), 100−102.
(54) Shields, E. P.; Krug, J. D.; Roberson, W. R.; Jackson, S. R.; Smeltz, M. G.; Allen, M. R.; Burnette, R. P.; Nash, J. T.; Virtaranta, L.; Preston, W.; Liberatore, H. K.; Wallace, M. A. G.; Ryan, J. V.; Kariher, P. H.; Lemieux, P. M.; Linak, W. P. Pilot-Scale Thermal Destruction of Per- and Polyfluoroalkyl Substances in a Legacy Aqueous Film Forming Foam. *ACS ES&T Eng.* **2023**, *3*, 1308−1317.
(55) Li, Q. E.; Zhang, B. J.; Lyu, S. S.; Qi, Z. Spontaneous Combustion Characteristics of Activated Carbon Modified via Liquid Phase Impregnation during Drying. *ACS Omega* **2023**, *8* (36), 32752−32764.
(56) Weber, N. H.; Delva, C. S.; Stockenhuber, S. P.; Grimison, C. C.; Lucas, J. A.; Mackie, J. C.; Stockenhuber, M.; Kennedy, E. M. Modeling and Experimental Study on the Thermal Decomposition of Perfluorooctanesulfonic Acid (PFOS) in an α-Alumina Reactor. *Ind. Eng. Chem. Res.* **2022**, *61* (16), 5453−5463.
(57) Zhang, J.; Gao, L.; Bergmann, D.; Bulatovic, T.; Surapaneni, A.; Gray, S. Review of Influence of Critical Operation Conditions on By-Product/Intermediate Formation during Thermal Destruction of PFAS in Solid/Biosolids. *Sci. Total Environ.* **2023**, *854*, 158796.
(58) Duchesne, A. L.; Brown, J. K.; Patch, D. J.; Major, D.; Weber, K. P.; Gerhard, J. I. Remediation of PFAS-Contaminated Soil and Granular Activated Carbon by Smoldering Combustion. *Environ. Sci. Technol.* **2020**, *54* (19), 12631−12640.
(59) 'Henrich, V.. In *The Surface Science of Metal Oxides 1994*; Cox, P. A., Ed.; Cambridge University Press, 1994; .
(60) Biswas, S.; Wong, B. M. Degradation of Perfluorooctanoic Acid on Aluminum Oxide Surfaces: New Mechanisms from Ab Initio Molecular Dynamics Simulations. *Environ. Sci. Technol.* **2023**, *57* (16), 6695−6702.
(61) Pacchioni, G.; Freund, H. Electron Transfer at Oxide Surfaces. the MgO Paradigm: From Defects to Ultrathin Films. *Chem. Rev.* **2013**, *113*, 4035−4072. June 12
(62) Tench, A. J.; Nelson, R. L. *Adsorbed Nitro-Compounds and Electron Donor Properties of Magnesium Oxide*; Royal Society of Chemistry, 1967; .
(63) Klabunde, K. J.; Nieves, I. Interaction of Activated Magnesium Oxide Surfaces with Spin Traps; ACS Publications, 1988; Vol. *92*, pp 2521−2525.. https://pubs.acs.org/sharingguidelines.
(64) Murphy, D. M.; Farley, R. D.; Purnell, I. J.; Rowlands, C. C.; Yacob, A. R.; Paganini, M. C.; Giamello, E. Surface Defect Sites Formed on Partially and Fully Dehydrated MgO: An EPR/ENDOR Study. *J. Phys. Chem. B* **1999**, *103* (11), 1944−1953.
(65) Garrone, E.; Zecchina, A.; Stone, F. S. An Experimental and Theoretical Evaluation of Surface States in MgO and Other Alkaline Earth Oxides. *Philos. Mag. B* **1980**, *42* (5), 683−703.
(66) Morris, R. M.; Klabunde, K. J.; Sager, F.; Fatiadi, A.; Parks, P. C.; white, D. G.; Perros, T. P.; Bockmair, G.; Fritz, P.; West, R.; Niu, Y.; Powell, D. L.; Evens, V.; Am Chem, J. *Introduction to the Principles of Heterogeneous Catalysis*; Electrochemical Society, 1983; Vol. *105*. https://pubs.acs.org/sharingguidelines.
(67) Sarasua, M.; Scott, E.; Helpem, J. A.; Ten Kortenaar, P. B. W.; Boggs, N. T., III; Pedersen, L. G.; Koehler, K. A.; Hiskey, R. G.; Morris, R. M.; Kaba, R. A.; Groshens, T. G.; Klabunde, K. J.; Baltisberger, R. J.; Woolsey, N. F.; Stenberg, V. I. *Nuclear Magnetic Resonance*; Elsevier, 1976; Vol. *3419*. https://pubs.acs.org/sharingguidelines.
(68) Orlando, R.; Millini, R.; Perego, G.; Dovesi, R. Catalytic Properties of F-Centres at the Magnesium Oxide Surface: Hydrogen Abstraction from Methane. *J. Mol. Catal. A: Chem.* **1997**, *119*, 253−262.
(69) Lin, S.-T.; Klabunde, K. J. Thermally activated magnesium oxide surface chemistry. Adsorption and decomposition of phosphorus compounds. *Langmuir* **1985**, *1*, 600−605. https://pubs.acs.org/sharingguidelines
(70) Ochs, D.; Braun, B.; Maus-Friedrichs, W.; Kempter, V. CO 2 Chemisorption at Ca and CaO Surfaces: A Study with MIES, UPS(HeI) and XPS. *Surf. Sci.* **1998**, *417*, 406−414.
(71) Ochs, D.; Brause, M.; Braun, B.; Maus-Friedrichs, W.; Kempter, V. CO 2 Chemisorption at Mg and MgO Surfaces: A Study with MIES and UPS(He I). *Surf. Sci.* **1998**, *397*, 101−107.
(72) Li, S.; Wang, C.; Luo, Z.; Zhu, X. Investigation on the Catalytic Behavior of Alkali Metals and Alkaline Earth Metals on the Biomass Pyrolysis Assisted with Real-Time Monitoring. *Energy Fuels* **2020**, *34* (10), 12654−12664.

https://doi.org/10.1021/acs.est.3c09795
Environ. Sci. Technol. XXXX, XXX, XXX−XXX

(73) Wang, W.; Lemaire, R.; Bensakhria, A.; Luart, D. Analysis of the Catalytic Effects Induced by Alkali and Alkaline Earth Metals (AAEMs) on the Pyrolysis of Beech Wood and Corncob. *Catalysts* **2022**, *12* (12), 1505.
(74) Case, P. A.; Truong, C.; Wheeler, M. C.; DeSisto, W. J. Calcium-Catalyzed Pyrolysis of Lignocellulosic Biomass Components. *Bioresour. Technol.* **2015**, *192*, 247−252.
(75) Li, H.; Wang, Y.; Zhou, N.; Dai, L.; Deng, W.; Liu, C.; Cheng, Y.; Liu, Y.; Cobb, K.; Chen, P.; Ruan, R. Applications of Calcium Oxide-Based Catalysts in Biomass Pyrolysis/Gasification - A Review. *J. Cleaner Prod.* **2021**, *291*, 125826.
(76) Lin, Y.; Zhang, C.; Zhang, M.; Zhang, J. Deoxygenation of Bio-Oil during Pyrolysis of Biomass in the Presence of CaO in a Fluidized-Bed Reactor. *Energy Fuels* **2010**, *24* (10), 5686−5695.
(77) Veses, A.; Aznar, M.; Martínez, I.; Martínez, J.; López, J.; Navarro, M. V.; Callén, M.; Murillo, R.; García, T. Catalytic Pyrolysis of Wood Biomass in an Auger Reactor Using Calcium-Based Catalysts. *Bioresour. Technol.* **2014**, *162*, 250−258.
(78) Alcazar-Ruiz, A.; Ortiz, M. L.; Sanchez-Silva, L.; Dorado, F. Catalytic Effect of Alkali and Alkaline Earth Metals on Fast Pyrolysis Pre-Treatment of Agricultural Waste. *Biofuels, Bioprod. Biorefin.* **2021**, *15* (5), 1473−1484.
(79) Wang, Z.; Mo, C.; Xu, S.; Chen, S.; Deng, T.; Zhu, W.; Wang, H. Ca(OH)2 Induced a Controlled-Release Catalytic System for the Efficient Conversion of High-Concentration Glucose to Lactic Acid. *Mol. Catal.* **2021**, *502*, 111406.
(80) Asikin-Mijan, N.; Lee, H. V.; Taufiq-Yap, Y. H.; Juan, J. C.; Rahman, N. A. Pyrolytic-Deoxygenation of Triglyceride via Natural Waste Shell Derived Ca(OH)2 Nanocatalyst. *J. Anal. Appl. Pyrolysis* **2016**, *117*, 46−55.
(81) Khachani, M.; Hamidi, A. E.; Halim, M.; Arsalane, S. Non-Isothermal Kinetic and Thermodynamic Studies of the Dehydroxylation Process of Synthetic Calcium Hydroxide Ca(OH) 2. *J. Mater. Environ. Sci.* **2014**, *5* (2), 615−624.
(82) Fraissler, G.; Jöller, M.; Brunner, T.; Obernberger, I. Influence of Dry and Humid Gaseous Atmosphere on the Thermal Decomposition of Calcium Chloride and Its Impact on the Remove of Heavy Metals by Chlorination. *Chem. Eng. Process* **2009**, *48* (1), 380−388.
(83) Yurkinskii, V. P.; Firsova, E. G.; Proskura, S. A. Thermal Dissociation of Sodium Hydroxide upon Evacuation. *Russ. J. Appl. Chem.* **2005**, *78*, 360−362.
(84) Liao, C.-J.; Lin, F.-H.; Chen, K.-S.; Sun, J.-S. Thermal Decomposition and Reconstitution of Hydroxyapatite in Air Atmosphere. *Biomaterials* **1999**, *20* (19), 1807−1813.
(85) Yamaguchi, N.; Masuda, Y.; Yamada, Y.; Narusawa, H.; Han-Cheol, C.; Tamaki, Y.; Miyazaki, T. Synthesis of CaO-SiO_2 Compounds Using Materials Extracted from Industrial Wastes. *Open J. Inorg. Non-Metallic Mater.* **2015**, *05* (01), 1−10.
(86) Yan, Z.; Wang, Z.; Liu, H.; Tu, Y.; Yang, W.; Zeng, H.; Qiu, J. Decomposition and Solid Reactions of Calcium Sulfate Doped with SiO2, Fe2O3 and Al2O3. *J. Anal. Appl. Pyrolysis* **2015**, *113*, 491−498.
(87) Weber, N. H.; Delva, C. S.; Stockenhuber, S. P.; Grimison, C. C.; Lucas, J. A.; Mackie, J. C.; Stockenhuber, M.; Kennedy, E. M. Thermal Decomposition of Perfluorooctanesulfonic Acid (PFOS) in the Presence of Water Vapor. *Ind. Eng. Chem. Res.* **2022**, *61* (41), 15146−15155.
(88) Uchimaru, T.; Tsuzuki, S.; Sugie, M.; Tokuhashi, K.; Sekiya, A. Ab Initio Study of the Hydrolysis of Carbonyl Difluoride (CF 2O): Importance of an Additional Water Molecule. *Chem. Phys. Lett.* **2004**, *396* (1−3), 110−116.
(89) Hao, S.; Choi, Y. J.; Wu, B.; Higgins, C. P.; Deeb, R.; Strathmann, T. J. Hydrothermal Alkaline Treatment for Destruction of Per-and Polyfluoroalkyl Substances in Aqueous Film-Forming Foam. *Environ. Sci. Technol.* **2021**, *55* (5), 3283−3295.
(90) Ram, H.; DePompa, C. M.; Westmoreland, P. R. Thermochemistry of Gas-Phase Thermal Oxidation of C_2 to C_8 Perfluorinated Sulfonic Acids with Extrapolation to C_{16}. *J. Phys. Chem. A* **2024**, *128*, 3387−3395.
(91) Weber, N. H.; Delva, C. S.; Stockenhuber, S. P.; Grimison, C. C.; Lucas, J. A.; Mackie, J. C.; Stockenhuber, M.; Kennedy, E. M. Thermal Mineralization of Perfluorooctanesulfonic Acid (PFOS) to HF, CO2, and SO2. *Ind. Eng. Chem. Res.* **2023**, *62* (2), 881−892.
(92) Weber, N. H.; Grimison, C. C.; Lucas, J. A.; Mackie, J. C.; Stockenhuber, M.; Kennedy, E. M. Influence of Reactor Composition on the Thermal Decomposition of Perfluorooctanesulfonic Acid (PFOS). *J. Hazard. Mater.* **2024**, *461*, 132665.
(93) Singh, R. K.; Fernando, S.; Baygi, S. F.; Multari, N.; Thagard, S. M.; Holsen, T. M. Breakdown Products from Perfluorinated Alkyl Substances (PFAS) Degradation in a Plasma-Based Water Treatment Process. *Environ. Sci. Technol.* **2019**, *53* (5), 2731−2738.
(94) Hao, S.; Choi, Y. J.; Wu, B.; Higgins, C. P.; Deeb, R.; Strathmann, T. J. Hydrothermal Alkaline Treatment for Destruction of Per-and Polyfluoroalkyl Substances in Aqueous Film-Forming Foam. *Environ. Sci. Technol.* **2021**, *55* (5), 3283−3295.
(95) Wang, F.; Shih, K.; Lu, X.; Liu, C. Mineralization Behavior of Fluorine in Perfluorooctanesulfonate (PFOS) during Thermal Treatment of Lime-Conditioned Sludge. *Environ. Sci. Technol.* **2013**, *47* (6), 2621−2627.
(96) Kim, T. H.; Lee, S. H.; Kim, H. Y.; Doudrick, K.; Yu, S.; Kim, S. D. Decomposition of Perfluorooctane Sulfonate (PFOS) Using a Hybrid Process with Electron Beam and Chemical Oxidants. *Chem. Eng. J.* **2019**, *361*, 1363−1370.
(97) Sasi, P. C.; Alinezhad, A.; Yao, B.; Kubátová, A.; Golovko, S. A.; Golovko, M. Y.; Xiao, F. Effect of Granular Activated Carbon and Other Porous Materials on Thermal Decomposition of Per- and Polyfluoroalkyl Substances: Mechanisms and Implications for Water Purification. *Water Res.* **2021**, *200*, 117271.
(98) Xiao, F.; Sasi, P. C.; Yao, B.; Kubátová, A.; Golovko, S. A.; Golovko, M. Y.; Soli, D. Thermal Stability and Decomposition of Perfluoroalkyl Substances on Spent Granular Activated Carbon. *Environ. Sci. Technol. Lett.* **2020**, *7* (5), 343−350.
(99) Trang, B.; Li, Y.; Xue, X.-S.; Ateia, M.; Houk, K. N.; Dichtel, W. R. Low-Temperature Mineralization of Perfluorocarboxylic Acids. *Science* **2022**, *377* (6608), 839−845. https://www.science.org
(100) Bentel, M. J.; Yu, Y.; Xu, L.; Li, Z.; Wong, B. M.; Men, Y.; Liu, J. Defluorination of Per- and Polyfluoroalkyl Substances (PFASs) with Hydrated Electrons: Structural Dependence and Implications to PFAS Remediation and Management. *Environ. Sci. Technol.* **2019**, *53* (7), 3718−3728.
(101) Yamada, T.; Taylor, P. H.; Buck, R. C.; Kaiser, M. A.; Giraud, R. J. Thermal Degradation of Fluorotelomer Treated Articles and Related Materials. *Chemosphere* **2005**, *61* (7), 974−984.
(102) Jollie, D. M.; Harrison, P. G. An in Situ IR Study of the Thermal Decomposition of Trifluoroacetic Acid. *J. Chem. Soc., Perkin Trans. 2* **1997**, 1571−1576.
(103) Blake, P. G.; Pritchard, H.; Blake, P. G.; Hole, K. J.; Soc, J. C.; Fawcett, F. S.; Tullock, C. W.; Coffman, D. D.; Amer, J.; Strouts, R. N.; Gilfillan, J. H.; Wilson, H. N.; Clark, H. C.; Willis, C. J. The Thermal Decomposition of TrifLuoroacetic Acid. *J. Chem. Soc. B* **1967**, *1*, 282.
(104) Blake, P. G.; Tomlinson, A. D.; Pritchard, H.; Chem, J. S.; Richard, H.; Chem, J. Thermal Decomposition of Fluoroacetic Acid. *J. Chem. Soc. B* **1971**, 1596−1597.
(105) Sandoval-Pauker, C.; Yin, S.; Castillo, A.; Ocuane, N.; Puerto-Diaz, D.; Villagrán, D. Computational Chemistry as Applied in Environmental Research: Opportunities and Challenges. *ACS ES&T Eng.* **2023**, *4*, 66−95.
(106) Li, Z.; Huang, H. H.; Huang, Y.; Huang, J.; Shen, M.; Zheng, J.; Wang, J. W.; Ouyang, G. Highly Efficient Electrochemical Oxidation of Hexafluoropropylene Oxide Homologues at a Boron-Doped Diamond Anode. *J. Environ. Chem. Eng.* **2023**, *11* (2), 109280.
(107) Chen, Y.; Bhati, M.; Walls, B. W.; Wang, B.; Wong, M. S.; Senftle, T. P. Mechanistic Insight into the Photo-Oxidation of Perfluorocarboxylic Acid over Boron Nitride. *Environ. Sci. Technol.* **2022**, *56* (12), 8942−8952.
(108) Bai, L.; Jiang, Y.; Xia, D.; Wei, Z.; Spinney, R.; Dionysiou, D. D.; Minakata, D.; Xiao, R.; Xie, H. B.; Chai, L. Mechanistic

https://doi.org/10.1021/acs.est.3c09795
Environ. Sci. Technol. XXXX, XXX, XXX−XXX

Understanding of Superoxide Radical-Mediated Degradation of Perfluorocarboxylic Acids. *Environ. Sci. Technol.* **2022**, *56* (1), 624−633.

(109) Pica, N. E.; Funkhouser, J.; Yin, Y.; Zhang, Z.; Ceres, D. M.; Tong, T.; Blotevogel, J. Electrochemical Oxidation of Hexafluoropropylene Oxide Dimer Acid (GenX): Mechanistic Insights and Efficient Treatment Train with Nanofiltration. *Environ. Sci. Technol.* **2019**, *53* (21), 12602−12609.

https://doi.org/10.1021/acs.est.3c09795
Environ. Sci. Technol. XXXX, XXX, XXX−XXX